Video Article

In Vivo Evaluation of Fracture Callus Development During Bone Healing in Mice Using an MRI-compatible Osteosynthesis Device for the Mouse Femur

Melanie Haffner-Luntzer[1], Fabian Müller-Graf[1,4], Romano Matthys[2], Alireza Abaei[3], René Jonas[1], Florian Gebhard[4], Volker Rasche*[3], Anita Ignatius*[1]

[1]Institute of Orthopedic Research and Biomechanics, University Medical Center Ulm

[2]RISystem

[3]Core Facility Small Animal MRI, University Medical Center Ulm

[4]Department of Traumatology, Hand-, Plastic-, and Reconstructive Surgery, University Medical Center Ulm

*These authors contributed equally

Correspondence to: Melanie Haffner-Luntzer at melanie.haffner-luntzer@uni-ulm.de

URL: https://www.jove.com/video/56679
DOI: doi:10.3791/56679

Keywords: Medicine, Issue 129, Fracture healing, femur osteotomy, MRI, external fixator, mouse model, callus development

Date Published: 11/14/2017

Citation: Haffner-Luntzer, M., Müller-Graf, F., Matthys, R., Abaei, A., Jonas, R., Gebhard, F., Rasche, V., Ignatius, A. *In Vivo* Evaluation of Fracture Callus Development During Bone Healing in Mice Using an MRI-compatible Osteosynthesis Device for the Mouse Femur. *J. Vis. Exp.* (129), e56679, doi:10.3791/56679 (2017).

Abstract

Endochondral fracture healing is a complex process involving the development of fibrous, cartilaginous, and osseous tissue in the fracture callus. The amount of the different tissues in the callus provides important information on the fracture healing progress. Available *in vivo* techniques to longitudinally monitor the callus tissue development in preclinical fracture-healing studies using small animals include digital radiography and µCT imaging. However, both techniques are only able to distinguish between mineralized and non-mineralized tissue. Consequently, it is impossible to discriminate cartilage from fibrous tissue. In contrast, magnetic resonance imaging (MRI) visualizes anatomical structures based on their water content and might therefore be able to noninvasively identify soft tissue and cartilage in the fracture callus. Here, we report the use of an MRI-compatible external fixator for the mouse femur to allow MRI scans during bone regeneration in mice. The experiments demonstrated that the fixator and a custom-made mounting device allow repetitive MRI scans, thus enabling longitudinal analysis of fracture-callus tissue development.

Video Link

The video component of this article can be found at https://www.jove.com/video/56679/

Introduction

Secondary fracture healing is the most common form of bone healing. It is a complex process mimicking specific aspects of ontogenic endochondral ossification[1,2,3]. The early fracture hematoma predominantly consists of immune cells, granulation and fibrous tissue. Low oxygen tension and high biomechanical strains hamper osteoblast differentiation at the fracture gap, but promote the differentiation of progenitor cells into chondrocytes[4,5,6]. These cells start to proliferate at the site of injury to form a cartilaginous matrix providing initial stability of the fractured bone. During callus maturation, chondrocytes become hypertrophic, undergo apoptosis, or trans-differentiate into osteoblasts. Neovascularization at the cartilage-to-bone transition zone provides elevated oxygen levels, allowing the formation of bony tissue[7]. After bony bridging of the fracture gap, biomechanical stability is increased and osteoclastic remodeling of the external fracture callus occurs to gain physiological bone contour and structure[3]. Therefore, the amounts of fibrous, cartilaginous, and bony tissue in the fracture callus provide important information about the bone healing process. Disturbed or delayed healing becomes visible by alterations of callus tissue development both in humans and mice[8,9,10,11]. Available *in vivo* techniques to longitudinally monitor callus tissue development in preclinical fracture healing studies using small animals include digital radiography and µCT imaging[12,13]. However, both techniques are only able to discriminate between mineralized and non-mineralized tissue. In contrast, MRI provides excellent soft tissue contrast and might therefore be able to identify soft tissue and cartilage in the fracture callus.

Previous work showed promising results for *post mortem* MRI in mice with articular fractures[14] and *in vivo* MRI in mice during intramembranous bone-defect healing[15]. However, both studies also stated limited spatial resolution and tissue contrast. We previously demonstrated the feasibility of high-resolution *in vivo* MRI for longitudinal assessment of soft callus formation during murine endochondral fracture healing[16]. Here, we report the protocol for using an MRI-compatible external fixator for femur osteotomy in mice in order to monitor callus tissue development longitudinally during the endochondral fracture healing process. The design of a custom-made mounting device for insertion of the external fixator ensured a standardized position during repeated scans.

Protocol

All animal experiments complied with international regulations for the care and use of laboratory animals and were approved by the regional regulatory authorities (No. 1250, Regierungspräsidium Tübingen, Germany). All mice were maintained in groups of two to five animals per cage on a 14-h light, 10-h dark circadian rhythm with water and food provided *ad libitum*.

1. Preparation of the Surgical Material and Pre-treatment of the Mice

1. Sterilize all surgical material. Use an autoclaving temperature of 120-135 °C for 20-30 min of sterilization time.
2. Purchase C57BL/6 mice or mice from another strain which are between 19-35 g of body weight. Follow the appropriate animal care and experimental protocols in accordance with national guidelines that is approved by the investigator's Institutional Animal Care and Use Committee. Allow a minimum of 7 days acclimatization period before starting the procedure.
3. Provide analgesia to all mice via the drinking water one day before surgery until the third postoperative day.

2. Surgical Procedure and Application of the External Fixator

1. Place the mouse into a tube preloaded with 5-7% isoflurane and 60 mL/min oxygen. After loss of postural reflexes, remove the mouse from the anesthesia induction tube and maintain the anesthesia via an inhalation mask providing 1-3% isoflurane and 60 mL/min oxygen.
    1. Monitor the breathing pattern and hind paw reflex during anesthesia. Ensure that the breathing rate is around 100 cycles/min and the hind paw reflex is absent.
    NOTE: The amount of gas needed is dependent on age, sex, body weight, and strain of the mouse.
2. Prior to surgery, inject the mouse with a single dose of antibiotics subcutaneously (clindamycin, 45 mg/kg). Furthermore, for maintenance of the physiological fluid balance, inject the mouse with a subcutaneous fluid depot of 500 µL saline (0.9% NaCl).
3. To prevent corneal drying, apply eye ointment to the mouse eyes. Place the mouse on a heating plate at 37 °C during the anesthesia and surgical procedure to maintain physiological body temperature.
4. Remove the fur from the right hind limb and scrub the surgical area with an alcohol-based disinfectant. Cover the right hind paw with a small part of a sterile glove to avoid unsterile areas. Disinfect the right hind limb three times. Place a sterile drape over the whole mouse except for the surgical area.
5. Incise the skin approximately 1 cm longitudinally along the anterior side of the right femur with a scalpel. Separate bluntly the *m. biceps femoris* and the *m. vastus lateralis* with micro scissor and forceps. Cut the tendon origin side at the femur trochanter with a micro scissor to allow free access to the anterolateral part of the bone. Make sure that the sciatic nerve is preserved.
6. Position the external fixator (axial stiffness of 3 N/mm, **Figure 1A**) parallel to the femur. Manually drill the boreholes through cortex with a 0.45-mm drill bit and place the ceramic mounting pins into the boreholes. Start with the most proximal pin, followed by the most distal pin, and the two pins in between.
    1. Make sure that there is no tension, compression, or shear stress on the fixator during the mounting procedure, otherwise the achieved osteotomy gap will not be sufficient due to relaxation of the fixator.
7. Humidify the bone with a small amount of sterile NaCl to avoid dehydration during the sawing procedure.
8. Create a 0.4-mm osteotomy through the whole bone between the two inner pins by using a 0.4 mm gigli wire saw.
NOTE: Optionally, an oscillating micro saw can be used to create the osteotomy. Make sure to avoid any metal chips from the saw at the osteotomy area.
9. Flush the osteotomy gap carefully with 2 mL of sterile NaCl to remove bone chips between the two fractured cortices.
10. Adapt the muscles by using a continuous suture with a resorbable suture (see **Table of Materials**). Then adapt the skin by using interrupted non-resorbable sutures (see **Table of Materials**). To avoid wound biting, do not place the suture at the cranial part of the wound.
NOTE: Do not use skin glue or clips since mice usually remove it from the wound causing further damage to the skin.
11. Clean the surgical area with a disinfectant and place the mouse into its cage. Monitor the mouse and supply sufficient heat (*e.g.* by infrared light) until it is fully awake. Monitor water, food intake, and body weight after the surgery to make sure the animal is not in pain and distress. Provide analgesia to all mice via the drinking water until the third postoperative day.
NOTE: Mice may be housed in groups of up to four animals.
12. Monitor the mouse's activity on days 1 to 5 after surgery. During that time course, the mouse should bear weight on the operated limb. Otherwise, the mouse must be excluded from further analysis.

3. MRI Procedure and Image Analysis

1. Prior to the MRI scanning procedure, anaesthetize the mouse according to the protocol in steps 2.1 and 2.3, and keep the respiratory rate around 100 cycles/min. Insert the external fixator at the right hind limb of the mouse carefully into a custom-made mounting device (**Figure 1B, C**).
    1. Make sure to avoid bending or compression of the fixator during this step since this may interfere with fracture healing.
    Note: The MRI scans can be conducted as early as 3 days after surgery, depending on the animal care and experimental protocol.
2. Place the mouse on a temperature controlled cradle for introduction into the MRI device. Attach the mounting device rigidly to the four-element head coil.
3. Acquire MRI data using a dedicated high-field small-animal MRI system operating at 11.7 T.
NOTE: The MRI data acquisition geometry is aligned with the femur bone, orthogonally to the screws.

1. Acquire data by applying a proton-density fat-suppressed multi-slice TSE sequence (PD-TSE) using acquisition parameters: echo/repetition time TE = 5.8 ms/TR = 2,500 ms, resolution $\Delta r = 52 \times 52 \times 350$ µm³, field-of-view (FOV) = 20 × 20 mm², and bandwidth $\Delta\omega$= 150 KHz.
2. NOTE: The total acquisition time for 22 slices is 36 min.

4. Open the acquired data with image analysis software. Enter the voxel size as 0.05 x 0.05 x 0.35 mm^3. Segment the different tissues in the fracture callus (bone, cartilage, fibrous tissue/bone marrow) based on their intensity with semi-automatic thresholding as follows.
   1. Click the "Edit New Label Field", click "Add Material", and rename the material to "callus". Distinguish the callus area from the surrounding tissues based on the hypo-intense signal from the periosteum using the "Lasso" tool.
   2. Click "add to material". Click "Add Material" and rename the material to "cartilage". Segment the cartilage by using the "threshold" tool and "Select only current material" from "callus". Click "cartilage" and "add to material". Repeat these steps with "bone" and "bone marrow/fibrous tissue".

5. Generate 3D reconstructions of the fractured femurs based on the tissue segmentation data using image analysis software. Click "Generate Surface", apply "None" for "Smoothing Type" and click "Surface View".
   NOTE: Very small, hyper-intense areas surrounding the ends of the fractured cortices are likely to be artifacts due to the transition from bony to soft tissue. These areas should be excluded from further analysis. Hyper-intense areas in the middle of the fracture callus during the endochondral phase of fracture healing represent cartilaginous tissue. Hypo-intense areas at the fracture callus distal from the osteotomy gap at the endochondral ossification phase and areas with the same intensity throughout the whole fracture callus at later healing stages represent newly formed bony callus tissue. Although these areas have a hypo-intense signal, the signal intensity from mature bone (cortex) is even lower. After thresholding the signal intensity for bony tissue and cartilaginous tissue in the fracture callus, mark the remaining tissue as bone marrow and fibrous tissue. Values for tissue segmentation are: bony tissue (including mature cortex, trabecular bone, and bony callus tissue) is segmented within the range of 1-3.3 (normalized signal intensity to mature cortex), bone marrow/fibrous tissue within the range of 3.4-5.4, and cartilaginous callus tissue within the range of 5.5-6.2.
6. If needed, repeat the MRI scan longitudinally during the fracture healing process. To monitor cartilaginous callus development, scan the mice on days 10, 14, and 21 after surgery.
   NOTE: The time points may depend on the animal care and experimental protocol.

Representative Results

First, the success of the surgical procedure can be confirmed by analysis of the MRI scans (see example in **Figure 2**). All four pins should be located in the middle of the femoral shaft. The size of the osteotomy gap should be between 0.3-0.5 mm. If the size of the osteotomy gap varies greatly from these values, the mouse should be excluded from further analysis.

Secondly, the evaluation of longitudinal scans during the fracture healing process in the same animal provides information about callus tissue development. If mice are scanned at day 10, 14, and 21 (see example in **Figure 3**), cartilaginous tissue is visible in the middle of the fracture callus on day 10 (relative cartilage area = 30.8%) and day 14 (relative cartilage area = 29.0%), and decreases until day 21 after surgery (relative cartilage area = 10.5%) (**Figure 3**). Bony tissue is visible at the periphery of the fracture callus on day 10 (relative bone area = 7.2 %), increases until day 14 (relative bone area = 15.6%), and body bridging occurs until day 21 (relative bone area = 45.7%).

Thirdly, after segmentation of the different tissues in the fracture callus using image analysis software, 3D images from the fractured femur and the fracture callus can be generated. In the example shown in **Figure 4**, a whole femur scanned on day 26 after fracture is displayed. Mature cortex is marked in grey, the ceramic pins are marked in yellow, callus soft tissue is marked in green, cartilage tissue is marked in red, and callus bony tissue is marked in purple.

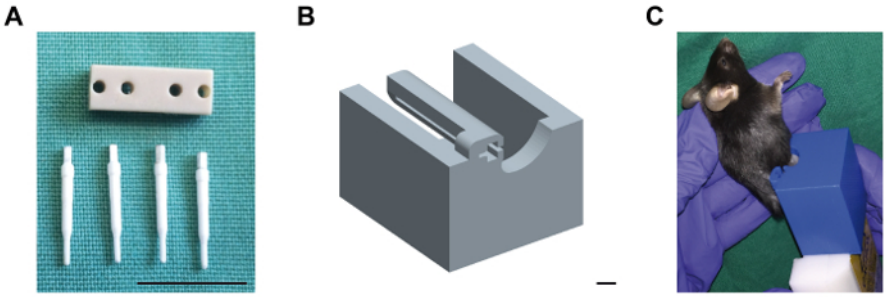

Figure 1: External fixator with ceramic mounting pins and MRI mounting device. (**A**) The plastic body of the external fixator is shown, as well as the four ceramic mounting pins which are compatible to MRI scans. Scale bar: 1 cm. (**B**) The computer-aided drawing of the custom-made mounting device for insertion of the external fixator during MRI scans is shown. The external fixator at the right femur of the mouse is inserted into the relief of the mounting device. Then, the device is plugged on the four-element head coil prior to scanning. Scale bar: 0.4 cm. (**C**) Mouse placed in the mounting device (blue), attached to the 4-element head coil (white). Please click here to view a larger version of this figure.

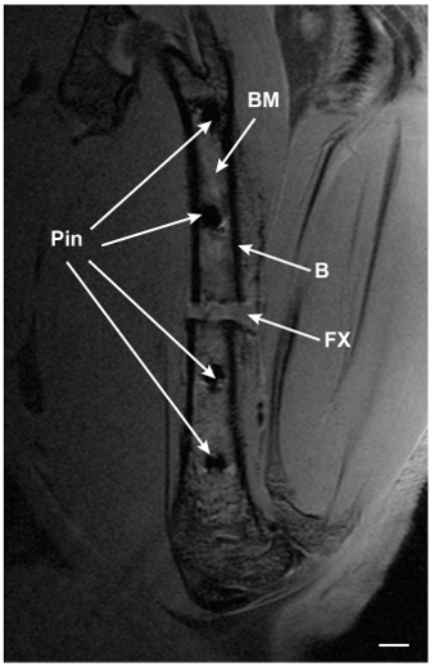

Figure 2: PD-TSE MRI image of a fractured femur 3 days after surgery. A central slice of a fractured femur scanned on day 3 after surgery is shown. BM: bone marrow; B: bone; FX: fracture gap. Scale bar: 0.5 mm. Please click here to view a larger version of this figure.

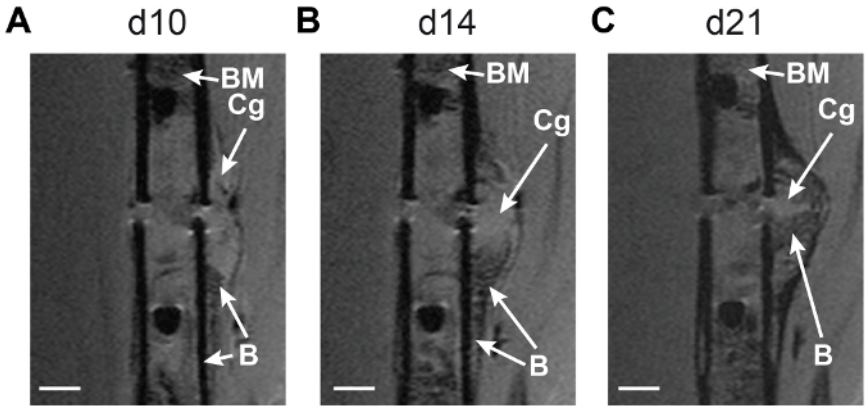

Figure 3: Longitudinal monitoring of fracture callus development using MRI technique. Central MRI slices from the fractured femur of one mouse scanned on (**A**) day 10, (**B**) day 14, and (**C**) day 21 after surgery are displayed. Hyper-intense cartilaginous tissue is visible in the middle of the fracture callus on day 10 and day 14, and decreases until day 21 after surgery. Hypo-intense bony tissue is visible at the periphery of the fracture callus on day 10, increases until day 14, and body bridging occurs until day 21. BM: bone marrow; Cg: cartilaginous tissue; B: bony tissue. Scale bar: 0.5 mm. Please click here to view a larger version of this figure.

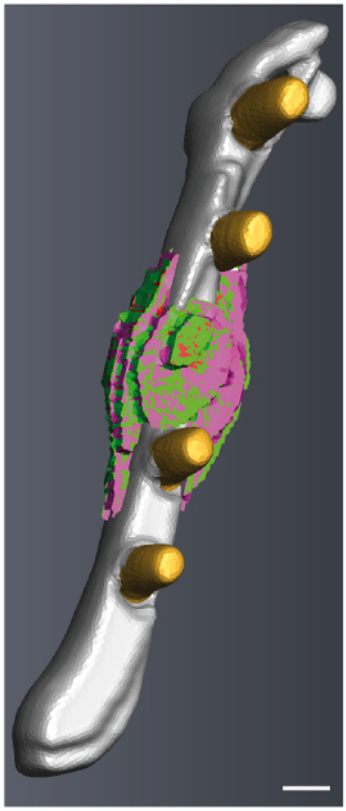

Figure 4: 3D reconstruction from a fractured femur scanned on day 26 after surgery. Mature cortex is marked in grey, the ceramic pins are marked in yellow, callus soft tissue is marked in green, cartilage tissue is marked in red, and callus bony tissue is marked in purple. The image was generated using image analysis software. Scale bar: 0.4 mm. Please click here to view a larger version of this figure.

Discussion

Modifications and Troubleshooting:

The main goal of this study was to describe a protocol for using of an MRI-compatible external fixator for femur osteotomy in the mouse with the ability to monitor callus tissue development longitudinally during the endochondral fracture-healing process. The design of a custom-made mounting device for insertion of the external fixator ensured a standardized position during repeated scans. Semi-automatic tissue segmentation allows the analysis of the amounts of fibrous, cartilaginous, and bony tissue in the fracture callus. Furthermore, 3D reconstructions of the MRI images allow visualization of the endochondral fracture healing process in each individual mouse.

Critical Steps Within the Protocol:

The most critical steps of the surgical procedure using the MRI-compatible external fixator are: (1) Avoid any damage to the sciatic nerve during the surgery, otherwise the mouse will not be able to weight bear within 5 days after the osteotomy and must be excluded from further analysis. (2) Avoid tension, compression, or shear stress on the fixator during the mounting procedure, otherwise the osteotomy gap will not have a standardized size and shape. Furthermore, make sure to mount the fixator parallel to the longitudinal axis of the femur, ensuring a stable fixation of the osteotomy. (3) Avoid metal chips from the saw if using a gigli wire saw, since those will interfere with the MRI scanning procedure.

The most critical steps of the MRI scanning procedure are: (1) Make sure to avoid bending or compression of the fixator during insertion and removal of the mounting device as this may interfere with fracture healing. (2) Ensure proper temperature control during the scanning procedure to maintain physiological body temperature.

Significance with Respect to Existing Methods and Limitations of the Technique:

Previous studies showed promising results for *post mortem* MRI in mice with articular fractures[14] and *in vivo* MRI in mice with intramembranous bone-defect healing[15]. However, both studies also stated limited spatial resolution and tissue contrast. We previously demonstrated the feasibility and accuracy of high-resolution *in vivo* MRI for longitudinal analysis of soft callus formation during the early and intermediate phases of fracture healing in mice by comparing the new MRI technique with the gold standards µCT and histomorphometry[16]. However, we also found that the spatial resolution of MRI is significantly lower than the resolution of *ex vivo* µCT. This is a clear limitation of the MRI technique when compared to competing techniques, including *ex vivo* but also *in vivo* µCT.

Future Applications:

Future perspectives for the use of MRI during murine fracture-healing studies are: (1) Combination of MRI scans with the use of contrast agents to measure blood flow through the injured limb. (2) Combination of MRI and PET scans, as well as labeling of cells with superparamagnetic particles of iron oxide for cell trafficking experiments[17,18,19,20].

Disclosures

The author Romano Matthys is an employee of RISystem AG Davos, Switzerland that produces the implants and implant specific instruments used in this article. All other authors have no competing financial interests.

Acknowledgements

We thank Sevil Essig, Stefanie Schroth, Verena Fischer, Katja Prystaz, Yvonne Hägele, and Anne Subgang for excellent technical support. We also thank the German Research Foundation (CRC1149, INST40/499-1) and the AO Trauma Foundation Germany for funding this study.

References

1. Claes, L., Recknagel, S., & Ignatius, A. Fracture healing under healthy and inflammatory conditions. *Nat Rev Rheumatol.* **8** (3), 133-143 (2012).
2. Einhorn, T. A. The cell and molecular biology of fracture healing. *Clin Orthop Relat Res.* (355 Suppl), S7-21 (1998).
3. Einhorn, T. A., & Gerstenfeld, L. C. Fracture healing: mechanisms and interventions. *Nat Rev Rheumatol.* **11** (1), 45-54 (2015).
4. Augat, P. *et al.* Local tissue properties in bone healing: influence of size and stability of the osteotomy gap. *J Orthop Res.* **16** (4), 475-481 (1998).
5. Claes, L. E., & Heigele, C. A. Magnitudes of local stress and strain along bony surfaces predict the course and type of fracture healing. *J Biomech.* **32** (3), 255-266 (1999).
6. Claes, L. E. *et al.* Effects of mechanical factors on the fracture healing process. *Clin Orthop Relat Res.* (355 Suppl), S132-147 (1998).
7. Hu, D. P. *et al.* Cartilage to bone transformation during fracture healing is coordinated by the invading vasculature and induction of the core pluripotency genes. *Development.* **144** (2), 221-234 (2017).
8. Hankenson, K. D., Zimmerman, G., & Marcucio, R. Biological perspectives of delayed fracture healing. *Injury.* **45 Suppl 2** S8-S15 (2014).
9. Meyer, R. A., Jr. *et al.* Age and ovariectomy impair both the normalization of mechanical properties and the accretion of mineral by the fracture callus in rats. *J Orthop Res.* **19** (3), 428-435 (2001).
10. Nikolaou, V. S., Efstathopoulos, N., Kontakis, G., Kanakaris, N. K., & Giannoudis, P. V. The influence of osteoporosis in femoral fracture healing time. *Injury.* **40** (6), 663-668 (2009).
11. Haffner-Luntzer, M., Kovtun, A., Rapp, A. E., & Ignatius, A. Mouse Models in Bone Fracture Healing Research. *Current Molecular Biology Reports.* **2** (2), 101-111 (2016).
12. Garcia, P. *et al.* Rodent animal models of delayed bone healing and non-union formation: a comprehensive review. *Eur Cell Mater.* **26** 1-14 (2013).
13. Histing, T. *et al.* Small animal bone healing models: standards, tips, and pitfalls results of a consensus meeting. *Bone.* **49** (4), 591-599 (2011).
14. Zachos, T. A., Bertone, A. L., Wassenaar, P. A., & Weisbrode, S. E. Rodent models for the study of articular fracture healing. *J Invest Surg.* **20** (2), 87-95 (2007).
15. Taha, M. A. *et al.* Assessment of the efficacy of MRI for detection of changes in bone morphology in a mouse model of bone injury. *J Magn Reson Imaging.* **38** (1), 231-237 (2013).
16. Haffner-Luntzer, M. *et al.* Evaluation of high-resolution In Vivo MRI for longitudinal analysis of endochondral fracture healing in mice. *PLoS One.* **12** (3), e0174283 (2017).
17. Beckmann, N., Falk, R., Zurbrugg, S., Dawson, J., & Engelhardt, P. Macrophage infiltration into the rat knee detected by MRI in a model of antigen-induced arthritis. *Magn Reson Med.* **49** (6), 1047-1055 (2003).
18. Al Faraj, A., Sultana Shaik, A., Pureza, M. A., Alnafea, M., & Halwani, R. Preferential macrophage recruitment and polarization in LPS-induced animal model for COPD: noninvasive tracking using MRI. *PLoS One.* **9** (3), e90829 (2014).
19. Rolle, A. M. *et al.* ImmunoPET/MR imaging allows specific detection of Aspergillus fumigatus lung infection in vivo. *Proc Natl Acad Sci U S A.* **113** (8), E1026-1033 (2016).
20. Niemeyer, M. *et al.* Non-invasive tracking of human haemopoietic CD34(+) stem cells in vivo in immunodeficient mice by using magnetic resonance imaging. *Eur Radiol.* **20** (9), 2184-2193 (2010).

